Bioorg. Med. Chem. Lett. 40 (2021) 127922

Contents lists available at ScienceDirect

Bioorganic & Medicinal Chemistry Letters

journal homepage: www.elsevier.com/locate/bmcl

Photodynamic activity and photoantimicrobial chemotherapy studies of ferrocene-substituted 2-thiobarbituric acid

Balaji Babu [a,b,*], Thivagar Ochappan [a], Thaslima Asraf Ali [a], John Mack [b], Tebello Nyokong [b], Mathur Gopalakrishnan Sethuraman [a,*]

[a] Department of Chemistry, The Gandhigram Rural Institute – Deemed to be University, Tamil Nadu 624 302, India
[b] Institute for Nanotechnology Innovation, Department of Chemistry, Rhodes University, Makhanda 6140, South Africa

ARTICLE INFO

Keywords:
Ferrocene
Metal to ligand charge transfer
Hydroxyl radical
Photodynamic Therapy
Photo-antimicrobial studies

ABSTRACT

A ferrocene-substituted thiobarbituric acid (**FT**) has been synthesized to explore its photophysical properties and photodynamic and photoantimicrobial chemotherapy activities. **FT** has an intense metal-to-ligand charge transfer (MLCT) band at *ca.* 575 nm. The ferrocene moiety of **FT** undergoes photooxidation to form a ferrocenium species which in turn produces hydroxyl radical in an aqueous environment, which was confirmed *via* the bleaching reaction of *p*-nitrosodimethylaniline (RNO). **FT** exhibits efficient PDT activity against MCF-7 cancer cells with an IC_{50} value of 5.6 μM upon irradiation with 595 nm for 30 min with a Thorlabs M595L3 LED (240 mW cm^{-2}). Photodynamic inactivation of *Staphylococcus aureus* and *Escherichia coli* by **FT** shows significant activity with log reduction values of 6.62 and 6.16 respectively, under illumination for 60 min at 595 nm. These results demonstrate that ferrocene-substituted thiobarbituric acids merit further study for developing novel bioorganometallic PDT agents.

Metallocenes have received considerable research interest in different fields owing to their interesting physical and chemical properties.[1–3] Ferrocene (Fc), an organometallic compound in which two π-bonded cyclopentadienyl (η^5-C_5H_5) ligands form a sandwich complex with a Fe(II) ion, is a suitable candidate for a wide range of applications in catalysis, electroactive materials, sensors, and in medicinal chemistry,[4–8] due to its facile functionalization and favorable electronic properties. Incorporation of Fc in various biologically active compounds has been found to enhance their activity. Chloroquine (CQ) an antimalarial drug is ineffective against certain strains of *Plasmodium falciparum* because of resistance developed by the malarial parasite. Interestingly, ferroquine (FQ), which is a ferrocenyl analogue of chloroquine, was found to be active against both CQ-sensitive and CQ-resistant strains of *Plasmodium falciparum*.[9,10] Ferrocifen is a ferrocene-appended analogue of tamoxifen, which is highly effective in both hormone-dependent (ER +) and hormone-independent (ER -) breast cancer, while in contrast, tamoxifen is active against only hormone-dependent (ER +) breast cancer.[11,12] This enhanced activity was attributed to the redox-active center of the ferrocene moiety. The ferrocenium (Fc^+) ion, which is the one-electron oxidized species of ferrocene, is known to exhibit an anti-proliferative effect on certain types of cancer cells.[13–15] Detailed mechanistic studies by electron paramagnetic resonance (EPR) spectroscopy have shown that ferrocenium salts degrade in an aqueous environment to undergo a Haber-Weiss-like cycle followed by a Fenton-type reaction generating highly reactive hydroxyl radicals (•OH), which exhibit cytotoxic effects on MCF-7 cells.[14,15]

The goal of this study is to develop a ferrocene-substituted thiobarbituric acid (**FT**) (Fig. 1a), which is expected to generate the ferrocenium moiety upon photoirradiation but remain inactive in the dark. The rationale for using the thiobarbituric acid is its ability to form hydrogen bonds through its carbonyl (C═O), thiocarbonyl (S═O), and NH groups with enzymes and proteins such as Sirtuins (Sirt2) and nicotinic acetylcholine receptor (nAChR), which can facilitate internalization of **FT** into cells.[16,17] Conjugating the ferrocene moiety to thiobarbituric acid forms a donor-π-acceptor (D-π-A) system. The optical spectra of ferrocene-based D-π-A systems usually contain an intense visible region intramolecular metal-to-ligand charge transfer (MLCT) band.[18–22] The photoinduced charge transfer process leads to the formation of a ferrocenium ion and an anion radical species.[23–26] The ferrocenium ion is expected to produce hydroxyl radical species, which is one of the active species in photodynamic therapy (PDT).[27,28] During PDT, a photosensitizer dye enters the S_1 state upon photoexcitation,

* Corresponding authors at: Department of Chemistry, The Gandhigram Rural Institute – Deemed to be University, Tamil Nadu 624 302, India.
E-mail addresses: balajibabu1900@gmail.com (B. Babu), mgsethu@gmail.com (M. Gopalakrishnan Sethuraman).

https://doi.org/10.1016/j.bmcl.2021.127922
Received 30 November 2020; Received in revised form 23 February 2021; Accepted 26 February 2021
Available online 8 March 2021
0960-894X/

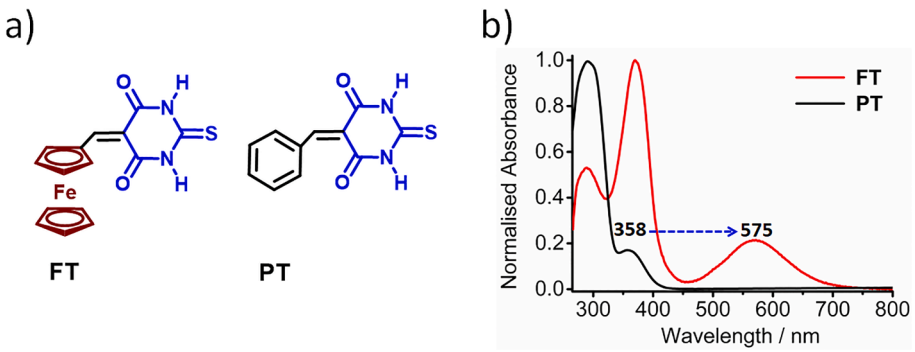

Fig. 1. The structure of the ferrocene conjugate that was studied in this work and that of the **PT** control compound; (b) UV–visible absorption spectra of **FT** and **PT** in 1:1 DMF/H_2O.

which undergoes intersystem crossing to the triplet manifold. The T_1 state can either undergo a Type-I process to form reactive oxygen species (ROS), such as $^{\bullet}OH$, $^{-\bullet}O_2$, or a Type-II process to transfer its energy to molecular oxygen to form $^1O_2$ species which are known to be toxic to surrounding tumor cells.[27,28] Photodynamic antimicrobial chemotherapy (PACT) follows the same principles of PDT. ROS formed by the photosensitizer dye cause oxidative damage to cell membrane integrity causing irreparable biological damage.[29,30] The key advantage of PACT over conventional chemotherapeutic drugs is that it is difficult for microorganisms to generate resistance against the ROS that are produced. The synthetic and non-linear optical (NLO) properties of **FT** have been reported in the literature,[31–33] and also it finds applications in wide fields,[34,35] but its potential application for PDT and PACT studies has not been explored. The objective of the present work is to synthesize and characterize **FT** (Fig. 1a) and to study its PDT activity towards MCF-7 cells and PACT activity against both Gram-positive *S. aureus* and Gram-negative *E. coli* bacteria. **PT** was used as a control compound to explore the effect of the ferrocenyl moiety on the PDT and PACT activity, (Fig. 1a).

FT and phenyl-substituted thiobarbituric acid (**PT**) were synthesized by condensation of 2-thiobarbituric acid with the corresponding aldehyde in ethanol in favorable yield.[31,32] The ^1H NMR spectrum of **FT** contains a peak at 8.25 ppm, which corresponds to the alkene proton. The signal for the unsubstituted cyclopentadienyl ring (η^5-C_5H_5) protons lies at 4.33 ppm. In contrast, signals of the substituted cyclopentadienyl ring η^5-C_5H_4 protons were observed at 5.04 and 5.39 ppm. The two NH protons lie at 12.08 and 12.19 ppm (Fig. S1). MALDI-TOF MS analysis of **FT** gave a molecular ion peak at 340.02 corresponding to a [M^+] species (Fig. S3).

The electronic absorption spectrum of the ferrocenyl conjugate **FT** along with its phenyl analogue (**PT**) in 1:1 DMF/H_2O is shown in Fig. 1b. **FT** has a band at 575 nm, which is absent in its precursor. This band arises from a metal-to-ligand charge-transfer (MLCT) transition from the ferrocene moiety to thiobarbituric acid. A similar type of charge transfer spectrum is observed in the literature for ferrocene-based D-π-A conjugates.[22,26] The MLCT band has a tail of absorbance to *ca.* 700 nm. This potentially enables red-light activation in the context of PDT applications. **PT**, which lacks a ferrocene moiety, has an absorption band at 378 nm and no absorption bands in the visible region. This demonstrates that the incorporation of the ferrocene moiety redshifts the MLCT absorption band. The absorption spectrum of **FT** measured in 1% DMF/PBS buffers does not exhibit any change in band morphology but the MLCT band is red-shifted to 585 nm (Fig. S5).

The structural optimization of **FT** was performed by density functional theory (DFT) calculations at the B3LYP/6-31G(d) level of theory. The energy-minimized structure is provided in the Supporting Information (Fig. S6). DFT and time-dependent DFT (TD-DFT) studies were performed to rationalize the electronic structures and photophysical properties of **FT** and related compounds. When a comparison is made between Fc, **FT**, and Fc-CHO (**FA**), there is a significant stabilization of the LUMO and slight stabilization of HOMO (Fig. S7). A calculated electronic excitation of **FT** at 592 nm corresponds to the experimentally observed band at 575 nm. This electronic excitation is associated with intramolecular charge transfer from the highest occupied molecular orbital (HOMO) of **FT** to the lowest unoccupied molecular orbital (LUMO). The HOMO and LUMO are localized predominantly on the ferrocenyl and thiobarbituric acid moieties, respectively (Fig. S7).[22,26] Thus, visible-light excitation is predicted to transfer an electron from the ferrocenyl moiety to the thiobarbituric acid which leads to the formation of a ferrocenium (Fc^+) ion with a ferric iron center which can generate hydroxyl radicals *via* Fenton-type reactions.[14,15,23–26]

For photoirradiation studies, a solution of **FT** in 1:1 DMF/H_2O was

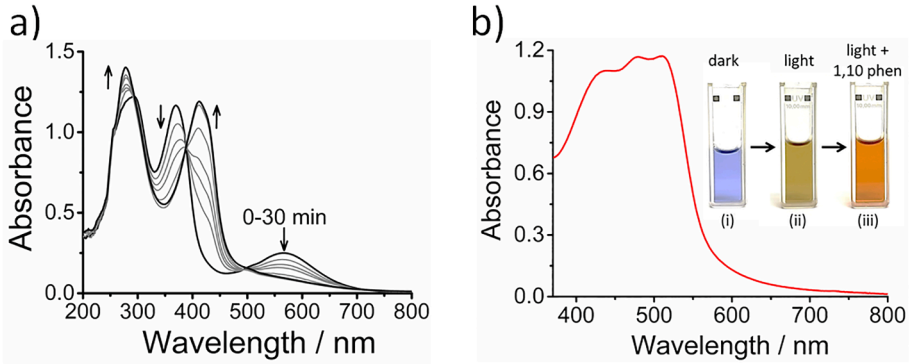

Fig. 2. (a) Changes in the UV–Visible spectra of **FT** on irradiating with 595 nm light for 0–30 min in 1:1 DMF/H_2O; (b) UV–Visible spectra of **FT** after irradiating for 30 min followed by addition of an excess of 1,10-phenanthroline. (Inset: Pictures of **FT** in dark, light irradiation for 30 min, light irradiation for 30 min followed by addition of 1,10-phenanthroline).

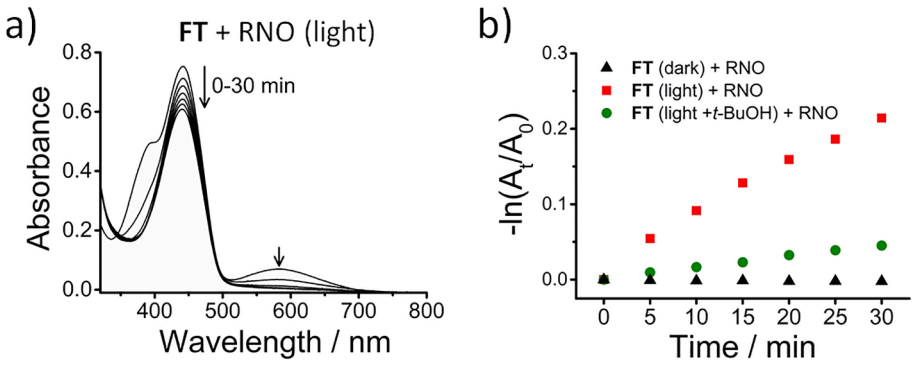

Fig. 3. (a) Change in the UV–visible absorption spectra of RNO with irradiation time (0–30 min) in the presence of **FT** in 1:1 DMF/Water; (b) Plot of the absorption change of RNO at 440 nm in the presence of **FT** in the dark (black triangle), light irradiation (red square), light irradiation + *t*-BuOH (green circle) in 1:1 DMF/H_2O.

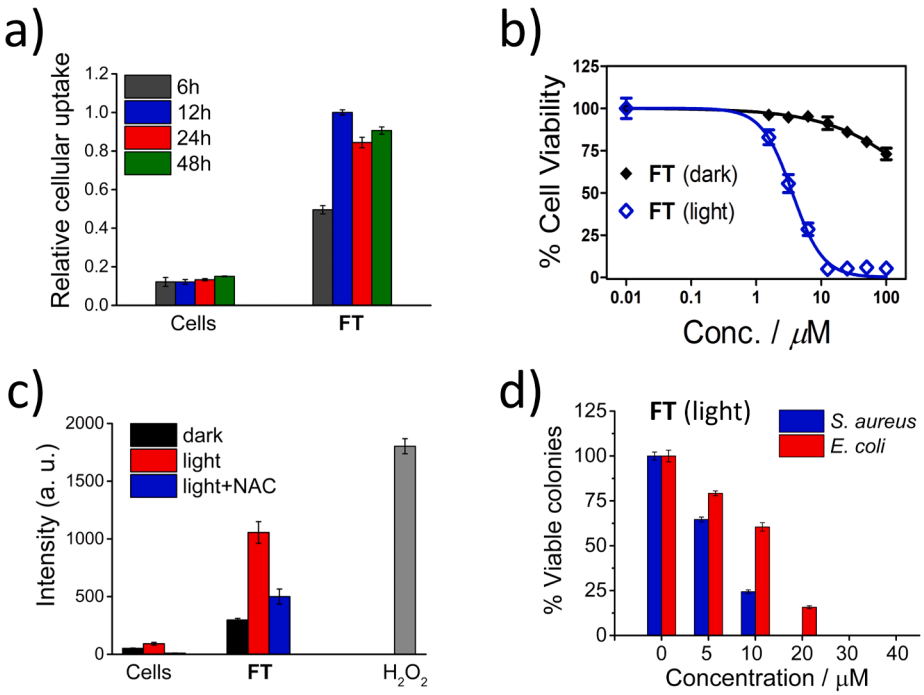

Fig. 4. (a) Cellular uptake of **FT** (5 μM) by MCF-7 cells with different time intervals (6, 12, 24, 48 h) measured by the absorption spectroscopy of lysed cells. (b) Cytotoxicity of **FT** against MCF-7 cells after 12 h incubation in the dark followed by photo-irradiation for 30 min with a Thorlabs M595L3 LED (240 mW cm^{-2}). (c) ROS detection in MCF-7 cancer cells produced by **FT** (5 μM) kept in the dark and upon illumination (H_2O_2 used as a +ve control). (d) Antimicrobial activities of **FT** towards *S. aureus* and *E. coli* on photoirradiation for 60 min at 595 nm with a Thorlabs M595L3 LED (240 mW cm^{-2}).

irradiated with a 595 nm LED (the same light source used for PDT/PACT studies) for 30 min to observe the effect of light irradiation, and its absorption spectra were recorded at regular time intervals (Fig. 2a). With increased irradiation time, a gradual decrease in the MLCT band (575 nm) and the band at 370 nm was observed with the appearance of new bands at 414 and 278 nm. This could be due to the formation of a ferrocenium (Fc^+) ion due to intramolecular charge transfer.[25,26] The color of the solution changes from blue to dark brown after 30 min of irradiation (inset Fig. 2b). The ferrocenium ions have been shown to undergo a consecutive chain of reaction in aqueous environments to form $^{\bullet}OH$, Fe^{2+}, and the cyclopentadienyl radical ($Cp^{\bullet}$).[14,15] When an excess of 1,10-phenanthroline (phen) is added to this irradiated solution, a red–orange color was immediately observed. The absorption spectrum of this solution is similar to that of $[Fe(Phen)_3]^{2+}$(Fig. 2b, Fig S8).[36] However, solutions of **FT** kept in the dark, and **PT** upon irradiation did not exhibit any apparent change in the visible region spectra.

The formation of $^{\bullet}OH$ radicals by **FT** on photo-irradiation is investigated by using *p*-nitrosodimethylaniline (RNO) as a hydroxyl radical quencher.[37,38] RNO is highly specific to hydroxyl radicals. The trapping of $^{\bullet}OH$ is easily monitored by monitoring its absorbance value at 440 nm. Solutions of the mixture of **FT** and RNO kept in the dark did not cause any change in the absorption spectra over time (Fig. S9). But when the solution of **FT** along with RNO is irradiated with 595 nm light, the absorbance at 440 nm corresponding to RNO decreased gradually with an increase in irradiation time (Fig. 3a). As expected, the band at 575 nm for **FT** also decreased in absorbance with increasing irradiation time. When the irradiation is performed in the presence of *t*-butanol as a $^{\bullet}OH$ quencher[39], the rate of decrease of RNO absorbance at 440 nm is reduced dramatically but still, the band at 575 nm for **FT** decreased, which provides evidence for the generation of $^{\bullet}OH$ by **FT** upon irradiation (Figs. 3b, S9). In contrast, the **PT** control compound did not cause any spectral changes with RNO either in the dark or under illumination (Fig. S10).

The intracellular uptake of **FT** in MCF-7 cells incubated with a 5 μM solution was measured by absorption spectroscopy of lysed cell extracts after different time intervals. Fig. 4a shows that **FT** is internalized effectively within 6 h, and the highest uptake is observed at 12 h. The dark toxicity of **FT** towards MCF-7 cells was tested by MTT assay after 12 h of incubation.[40] Since **FT** is insoluble in water, the addition of **FT** to the cell culture required preliminary solubilization in DMSO to form stock solutions that were then diluted to different concentrations with DMEM media. The final concentration of DMSO was always < 0.5%.

Table 1
Photophysical data of **FT** in 1:1 DMF/H_2O and its cytotoxicity data in MCF-7 cells and PACT data on *S. aureus* and *E. coli.*

		FT
λ_{max}/nm ($\varepsilon \times 10^3$ $M^{-1}cm^{-1}$)		370 (15.9), 575 (3.7)
IC_{50} (μM)	Dark [a]	> 100
	Light [b]	5.6 (±0.9)
Log red[c] (MBC / μM)[d]	*S. aureus*	6.62 (20)
	E. coli	6.16 (30)

[a] 12 h incubation in MCF-7 cells in the dark, [b]12 h incubation in MCF-7 cells in the dark followed by exposure to a Thorlabs M595L3 LED (240 mW cm^{-2}) for 30 min, [c]Log reduction values for the photoinactivation effects of **FT** (15 and 25 μM for *S. aureus* and *E. coli*, respectively) after 60 min irradiation at 595 nm with a Thorlabs M595L3 LED (240 mW cm^{-2}), [d] Minimum bactericidal concentration (MBC).

Upon photoirradiation with a 595 nm LED, MCF-7 cells incubated with **FT** exhibited significant cytotoxicity effects with an IC_{50} value (concentration required for 50% inhibition of cell proliferation) of 5.6 μM (Fig. 4b, Table 1). **FT** treated cells that were kept in the dark exhibited no significant cytotoxicity (IC_{50} > 100 μM). Fig. 4b contains the dose–response curves for **FT** in the dark and under illumination. Control experiments with **PT** exhibited no cytotoxicity in the dark or when irradiated (data not shown). The 2′,7′-dichlorofluorescein diacetate (DCFDA) assay was performed to provide direct evidence for intracellular ROS formation.[41] MCF-7 cells treated with **FT** exhibited a significant increase in 2′,7′-dichlorofluorescein fluorescence intensity when irradiated with light when a comparison is made to the response of the dark treated cells (Fig. 4c). When irradiation was carried out in the presence of *N*-acetyl cysteine (NAC), a ROS scavenger, the fluorescence intensity decreased, which indicates the involvement of reactive oxygen species.

The photoantimicrobial chemotherapy activity of **FT** was also assessed against *S. aureus* (Gram-positive) and *E. coli* (Gram-negative). The PACT studies were performed by the surface plating method.[42,43] To optimize the concentration selected for further studies, bacterial survival experiments were carried out at various concentrations of **FT** by irradiating with a Thorlabs M595L3 LED (240 mW cm^{-2}) for 60 min. Fig. 4d demonstrates that as anticipated the % bacterial viability decreased significantly with increased **FT** concentration, and no viable bacterial colonies were found at higher concentrations. These experiments established minimum bactericidal concentration (MBC) for **FT** of 20 and 30 μM against *S. aureus* and *E. coli,* respectively. Based on the above results, concentrations of 15 and 25 μM were selected for *S. aureus* and *E. coli*, respectively, to determine the PACT activity of **FT** in terms of log reduction (log red). PACT studies were performed at different time intervals (0–60 min). The log CFU (colony forming units) *vs* irradiation time plot is shown in Fig. S11. Log reduction values of 6.62 and 6.16 were obtained for *S. aureus* and *E. coli*, respectively, using the formula:

$$log\ reduction = log_{10}(A_0) - log_{10}(A_{60})$$

where A_0 and A_{60} are the number of viable micro-organisms at 0 and 60 min of light treatment, respectively. **FT** treated *S. aureus* and *E. coli* did not exhibit a reduction in bacterial viability in the absence of light treatment (Fig. S12). As expected, during control experiments with **PT**, ferrocene carboxaldehyde (**FA**) remained inactive due to the absence of any absorption band at the wavelength used for irradiation (Fig. S13). Photosensitizers with 3 log reduction or above are considered as antibacterial agent.[44]

A ferrocene-substituted thiobarbituric acid was successfully prepared and characterized. **FT** has an intense MLCT band centered at *ca.* 575 nm in 1:1 DMF/H_2O. The ability of **FT** to generate the $^{\bullet}OH$ radical upon photoirradiation was studied *via* the bleaching reaction of RNO. Significant photocytotoxicity with an IC_{50} value of 5.6 μM was observed against MCF-7 cells upon irradiation at 595 nm with a Thorlabs M595L3 LED. The dye remained inactive in the dark, however. The DCFDA assay provided direct evidence for the generation of intracellular ROS upon light irradiation. **FT** was found to have significant PACT activity against *S. aureus* and *E. coli* with high log reduction values. The results demonstrate that **FT** has the potential to be developed further as a photosensitizer dye for PDT and PACT. Further studies are in progress to structurally modify ferrocene-based D-π-A conjugates to improve their aqueous solubility so they can be further evaluated in PDT studies.

Declaration of Competing Interest

The authors declare that they have no known competing financial interests or personal relationships that could have appeared to influence the work reported in this paper.

Acknowledgements

Theoretical calculations were carried out at the Centre for High Performance Computing in Cape Town. Thanks are due to the authorities of GRI-DTBU for encouragement and UGC-SAP for financial support.

Appendix A. Supplementary data

Supplementary data to this article can be found online at https://doi.org/10.1016/j.bmcl.2021.127922.

References

1 Janiak C. *Coord Chem Rev*. 2006;250:66–94.
2 Janiak C, Blank F. *Macromol Symp*. 2006;236:14–22.
3 Sha Y, Zhang Y, Xu E, et al. *Chem Sci*. 2019;10:4959–4965.
4 Khan A, Wang L, Yu H, et al. *Appl Organomet Chem*. 2018;32, e4575.
5 Sun R, Wang L, Yu H, et al. *Organometallics*. 2014;33:4560–4573.
6 Wei Z, Wang D, Liu Y, et al. *J Mater Chem C*. 2020;8:10774–10780.
7 Santos MM, Bastos P, Catela I, Zalewska K, Branco LC. *Mini-Reviews Med. Chem.* 2017;17:771–784.
8 Wang R, Chen H, Yan W, Zheng M, Zhang T, Zhang Y. *Eur J Med Chem*. 2020;190, 112109.
9 Biot C, Glorian G, Maciejewski LA, et al. *J Med Chem*. 1997;40:3715–3718.
10 Kondratskyi A, Kondratska K, Vanden Abeele F, et al. *Sci Rep*. 2017;7:15896.
11 Top S, Tang J, Vessières A, Carrez D, Provot C, Jaouen G. *Chem Commun*. 1996:955–956.
12 Jaouen G, Vessières A, Top S. *Chem Soc Rev*. 2015;44:8802–8817.
13 Tamura H, Miwa M. *Chem Lett*. 1997;26:1177–1178.
14 Osella D, Ferrali M, Zanello P, et al. *Inorganica Chim Acta*. 2000;306:42–48.
15 Tabbì G, Cassino C, Cavigiolio G, et al. *J Med Chem*. 2002;45:5786–5796.
16 Arias HR, McCardy EA, Gallagher MJ, Blanton MP. *Mol Pharmacol*. 2001;60:497–506.
17 Uciechowska U, Schemies J, Neugebauer RC, et al. *ChemMedChem*. 2008;3:1965–1976.
18 Tahara K, Akehi S, Akita T, Katao S, Kikuchi J, Tokunaga K. *Dalt Trans*. 2015;44:14635–14645.
19 David E, Thirumoorthy K, Palanisami N. *Appl Organomet Chem*. 2018;32, e4522.
20 Garra P, Brunel D, Noirbent G, et al. *Polym Chem*. 2019;10:1431–1441.
21 Brunel D, Noirbent G, Dumur F. *Dye Pigment*. 2019;170, 107611.
22 Prabu S, David E, Viswanathan T, et al. *J Mol Struct*. 2020;1202, 127302.
23 Fery-Forgues S, Delavaux-Nicot B. *J Photochem Photobiol A Chem*. 2000;132:137–159.
24 Fukuzumi S, Okamoto K, Yoshida Y, Imahori H, Araki Y, Ito O. *J Am Chem Soc*. 2003;125:1007–1013.
25 Maity B, Chakravarthi BVSK, Roy M, Karande AA, Chakravarty AR. *Eur J Inorg Chem*. 2011;2011:1379–1386.
26 Balaji B, Balakrishnan B, Perumalla S, Karande AA, Chakravarty AR. *Eur J Inorg Chem*. 2015;2015:1398–1407.
27 Ethirajan M, Chen Y, Joshi P, Pandey RK. *Chem Soc Rev*. 2011;40:340–362.
28 dos Santos AF, de Almeida DRQ, Terra LF, Baptista MS, Labriola L. *J Cancer Metastasis Treat*. 2019;5:25.
29 Wainwright M, Maisch T, Nonell S, et al. *Lancet Infect Dis*. 2017;17:e49–e55.
30 Maldonado-Carmona N, Ouk T-S, Calvete MJF, Pereira MM, Villandier N, Leroy-Lhez S. *Photochem Photobiol Sci*. 2020;19:445–461.
31 Asiri AM. *Appl Organomet Chem*. 2001;15(11):907–915.
32 Pal SK, Krishnan A, Das PK, Samuelson AG. *J Organomet Chem*. 2001;637–639:827–831.
33 Stankovic E, Toma S, Van Boxel R, Asselberghs I, Persoons A. *J Organomet Chem*. 2001;637–639:426–434.
34 Xu L, Chu Z, Wang H, et al. *ACS Appl Bio Mater*. 2019;2(8):3429–3438.
35 Xu L, Wang H, Chu Z, et al. *ACS Appl Polym Mater*. 2020;2(2):741–750.
36 Agustina E, Goak J, Lee S, Seo Y, Park J-Y, Lee N. *ChemistryOpen*. 2015;4:613–619.

37 Kraljić I, Trumbore CN. *J Am Chem Soc*. 1965;87:2547–2550.
38 Santos JEL, Antonio Quiroz M, Cerro-Lopez M, de Moura DC, Martínez-Huitle CA. *New J Chem*. 2018;42:5523–5531.
39 Kozmér Z, Takács E, Wojnárovits L, Alapi T, Hernádi K, Dombi A. *Radiat Phys Chem*. 2016;124:52–57.
40 Berridge MV, Herst PM, Tan AS. *Biotechnol Annu Rev*. 2005;11:127–152.
41 Oparka M, Walczak J, Malinska D, et al. *Methods*. 2016;109:3–11.
42 Sindelo A, Kobayashi N, Kimura M, Nyokong T. *J Photochem Photobiol A Chem*. 2019;374:58–67.
43 Osifeko OL, Uddin I, Mashazi PN, Nyokong T. *New J Chem*. 2016;40:2710–2721.
44 Alves E, Faustino MAF, Neves MG, Cunha A, Tome J, Almeida A. *Fut Med Chem*. 2014;6:141–164.